

Protonation effects on the photophysical properties of poly(2,5-pyridine diyl)

A. P. Monkman,^{a)} M. Halim, I. D. W. Samuel, and L. E. Horsburgh
*Organic Electroactive Materials Research Group, Rochester Building, Department of Physics,
University of Durham, South Road, Durham DH1 3LE, United Kingdom*

(Received 3 April 1998; accepted 9 September 1998)

We have recently shown that poly(2,5-pyridine diyl) (PPY) can be synthesized to yield a polymer with high photoluminescence quantum yield (PLQY) in the solid state, and that it is an excellent electron transport material. To explore the photophysical properties of PPY further, we have used a range of acidic “dopants” to protonate the nitrogen sites on each ring and made observations on how this affects the optical properties of the resultant protonated PPY films. In general, we find that sulphonic acids have the greatest effect, causing perturbations to both the ground-state and excited-state properties of the PPY. These changes occur with only moderate reduction of the PLQY, whereas nonsulphonic acids cause a larger reduction in PLQY without significantly affecting the ground- or excited-state energy levels. These aspects of the photophysics of PPY can be described using a simple ring torsion argument. This model can also account for the observed shifts between solution state and solid-state emission wavelengths. © 1998 American Institute of Physics. [S0021-9606(98)70147-3]

I. INTRODUCTION

The first report of electroluminescence (EL) in poly(*p*-phenylenevinylene) (PPV)¹ has rejuvenated the field of conjugated polymers, encouraging the synthesis of many new and exciting polymers and allowing physicists the opportunity to use even more esoteric spectroscopic techniques to investigate them. The flexibility of polymer synthesis and processing² combined with chemical tuning of properties via novel monomer synthesis is one of the great attractions of the conjugated polymers. However, there is still a major concern over the oxidative and photostability of the active polymers in light emitting or photovoltaic devices. For example, to attain the lifetime requirements demanded by industry i.e., 10 000 h operating lifetime for LEDs, is very demanding for the current first generation of luminescent polymers. Thus there has been a drive to synthesize more stable luminescent polymers which are still highly efficient and can be processed in the same simple fashion as the current materials. This problem originally led us to investigate poly(2,5-pyridine diyl) (PPY).

From a simple chemical standpoint the reason for the oxidative instability of conjugated polymers arises from the electron rich π orbitals which are relatively easy to oxidize. To the physicist, of course, this is why these materials are so interesting since they can be easily manipulated by redox chemistry to yield, for example, a conductive state. One methodology for the design of the next generation of luminescent polymers is to make the process of oxidation more difficult while retaining sufficient π electron density to impart the desired physics. This can be achieved by introducing heteroatoms into the π system of the repeat unit i.e., replac-

ing a phenyl ring carbon atom with a nitrogen atom in the case of PPY, the structure of which is depicted in Fig. 1. This polymer and its basic properties were first reported by Yamamoto *et al.*³ They found that PPY (and substituted variants of the polymer) is luminescent, and indeed very stable with respect to oxidation. In fact they were unable to oxidize the polymer electrochemically even under severe conditions. PPY can, however, be reduced (*n*-doped) to yield a conductive form. Therefore, the PPY family of polymers seems an ideal starting place to find the next generation of conjugated polymers for light emitting diode (LEDs) applications. Recently we have shown that improved synthesis can yield PPY with high solid-state PL quantum yield, 30%⁴ which we have further improved to $37 \pm 3\%$. LEDs can be fabricated from PPY but only have moderate EL efficiency at present.^{5,6} Unlike any other luminescent conjugated polymer, PPY is found to have a PLQY in the solid state (37%) which is twice that measured in solution (17%), making this polymer unique at present and a most promising and intriguing material.

Initial studies of the photophysics of PPY have shown that in formic acid solution, the polymer emits in the blue (470 nm), whereas in the solid state the emission band red-shifts considerably (560 nm), yielding emission in the green, see Fig. 2. As can be seen, there are large shifts between the peak positions of both the absorption and PL bands in solution and solid state, with the solid state showing a greater shift. These first studies, however, only reported poor solid-state PLQY levels, typical of order 5%, which were lower than that estimated for the solution state. These findings led the authors to the natural conclusion that emission in the solid state originated from either aggregate or excimer states^{3,7} i.e., intermolecular interactions dominated the photophysics of PPY in the solid state. The difference between

^{a)} Author to whom correspondence should be addressed; electronic mail: a.p.monkman@durham.ac.uk

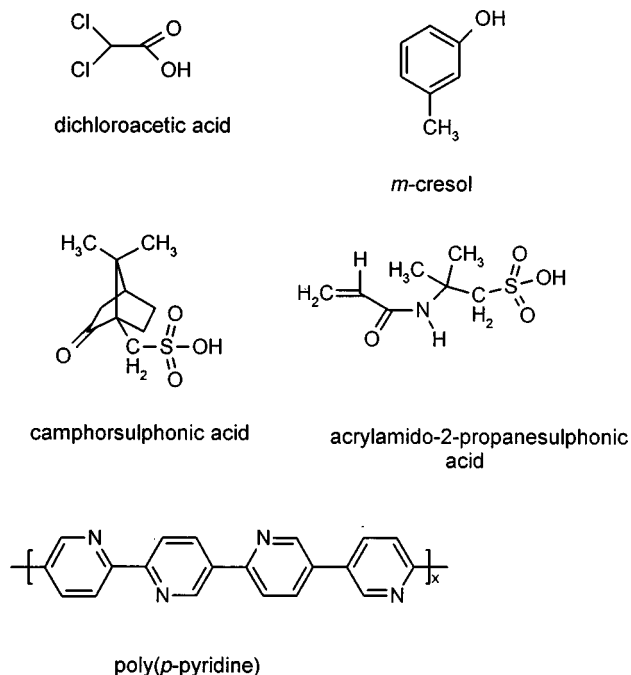


FIG. 1. Schematic structure of poly(*p*-pyridine) and various acids used to protonate the polymer in this work.

these states is that the interchain interaction occurs between two chains in their ground states in the case of aggregation, whereas the interaction occurs between a chain in its excited state and a chain in the ground state in the case of the excimer i.e., excited dimer. Therefore, spectroscopically there should be clear differences between the two. Concentration dependent solution state PL does not reveal a characteristic coexistence of excimer and monomer emission at any concentration⁶ unlike classic excimer systems such as the methyl anthracenes.⁸ This, coupled with the fact that there are observable changes in the absorption band profile between solution and solid which are not seen even in very high concentration solutions and the fact that PLQY is higher in the solid state than solution state, suggest that neither excimers nor aggregation are the correct interpretation of the experimental data.

To elucidate this further we have studied the effect of diluting PPY in a host polymer matrix, polymethylmethacry-

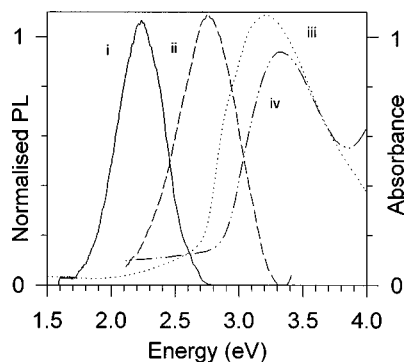


FIG. 2. Absorption and emission spectra of poly(*p*-pyridine) in both solution and solid state: (i) solid-state emission; (ii) solution state emission; (iii) solid-state absorption; (iv) solution state absorption.

late (PMMA).⁶ Here we find a progression from solid-statelike emission to solution like emission upon dilution. At levels of 10 000 to 1 (PMMA/PPY) emission is substantially in the blue.⁹ Excitation profiles suggest two emission centers, corresponding to a “solution state” and the “solid state,” although this work cannot unambiguously differentiate between the proposed theories. Thus we have devised another way of investigating the photophysics of this most intriguing polymer. Using polyaniline (PANi) as a model, we know that functionalized sulphonic acids impart very different properties to the polymer as compared to inorganic Brønsted acids.^{10–12} One main influence is the hydrogen bonding of the counter ion which dictates crystal structure and many physical properties of PANi^{12,13} and also their strong acidic nature in weak organic acid solvents means that we can use them with the PPY system. Therefore, we have chosen a range of functionalized and nonfunctionalized acids, which are soluble in formic acid, to protonate the PPY in formic acid solution from which films can be spun. The acids, both strong and weak, remain in the films after evaporation and in some cases protonation of the PPY nitrogen sites can clearly be seen using x-ray photoemission spectroscopy (XPS).¹⁴ Our main intention was to alter the spacing between adjacent rigid PPY chains and thus affect any interchain states. It has been calculated that the nitrogen lone pair electrons play no part in the aromatic π ring system^{15,16} (for a nearly planar chain conformation) and that protonation only affects deep lying (σ bond) states, not the frontier orbitals, thus having no direct effect on the highest occupied molecular orbital–lowest unoccupied molecular orbital (HOMO–LUMO) transition or emission process.¹⁶ In this paper we shall report on the effects of protonation on absorption, photoluminescence, and photoluminescence quantum yield in the solid state. A new model will be put forward to explain both our current observations and some of the other photophysical properties of PPY.

II. EXPERIMENT

Poly(2,5-pyridinediyl) is prepared by dehalogenation polycondensation of 2,5-dibromopyridine with tetrakis(triphenylphosphine)nickel(0) prepared *in situ* from reduction of NiCl_2 by Zn in the presence of PPh_3 in N,N-dimethylformamide (DMF).^{17,18} In a typical preparation, zinc (0.75 g, 11.5 mmol), nickel chloride (2.09 g, 16.4 mmol), triphenylphosphine (4.48 g, 17.1 mmol), and dibromopyridine (2.07 g, 8.74 mmol) were weighed into a flask which had been flushed with nitrogen. Nitrogen-purged DMF (20 ml) was added, and the reaction was heated to 70°C for 16 h. Acetone (100 ml) was added, and the crude product was isolated by filtration. The product was purified by stirring successively in hot aqueous solutions of $\text{Na}_4(\text{edta})$, edta, and $\text{Na}_4(\text{edta})$ (edta=ethylenediaminetetraacetic acid). The product was isolated with a yield of 0.64 g (95%). Polymer molecular weight was determined both by gel permeation chromatography (GPC) and light scattering. Both yield a Mw of 6000 daltons (80 repeat units), polydispersity of 1.7 and confirm that the polymer is a rigid rod.¹⁹ x-ray powder diffraction reveals the as synthesized PPY powder to be >80% crystalline reflecting the rigid rod nature and low polydispersity

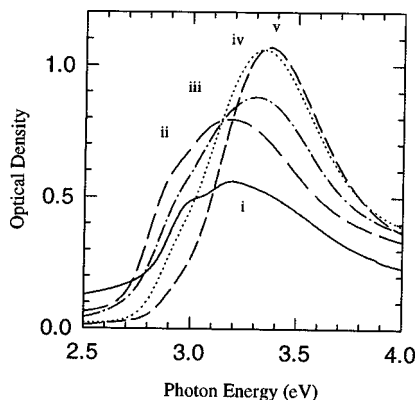


FIG. 3. Absorption spectra of poly(*p*-pyridine) as a function of CSA doping level: (i) 0%, (ii) 25%, (iii) 50%, (iv) 75%, and (v) 100% CSA content.

sity of our polymer.¹⁹ Thin films of the polymer were typically spin coated onto Spectrosil discs of 12 mm diam from a 20 mg.ml⁻¹ solution in formic acid. The absorption peak of these films was at 360 nm whereas the PL peak was at 540 nm.

The doping acids used were camphorsulphonic acid (CSA), 2-acrylamido-2-methyl-1-propanesulphonic acid (AMPSA), dichloroacetic acid (DCA) and *m*-cresol, the structure of these acids is shown in Fig. 1. These were added in molar ratios to PPY such that doping levels of 25%, 50%, 75%, and 100% were nominally achieved. As with PANi, 50% implies that one acid molecule was added for every two PPY repeat units i.e., theoretically half of the nitrogens present should be protonated. Polymer and acid were dissolved in formic acid, such that solutions were effectively 20 mg.ml⁻¹ with respect to the PPY. This helps to maintain high quality film formation with maximum optical absorbance of ~ 1 throughout. Films were spun onto glass and quartz substrates at 3500 rpm for 30 s. Absorption spectra were measured using a Perkin Elmer $\lambda 19$ spectrophotometer. Luminescence spectra were measured using a Jobin-Yvon CCD spectrograph with excitation provided by the ultraviolet (UV) lines of an argon ion laser (360–380 nm). PL quantum yield measurements were made using an integrating sphere to collect all the emitted light, following a similar methodology to Greenham *et al.*,²⁰ as described previously.⁴ Solution state measurements were made in both the integrating sphere and by conventional comparison to the laser dye quinine sulphate. Both techniques yield a PLQY value of $17 \pm 3\%$.

III. RESULTS

A. PPY:CSA

Absorption spectra versus CSA content are shown in Fig. 3, which also includes a spectrum of the pristine PPY for comparison. From the pristine PPY solid-state absorption spectrum three features can clearly be observed. For ease of discussion, changes to these will be referred to throughout the following discussion. These are denoted the low-energy shoulder (LES) which is observed at 3.0 eV, absorption band maximum (ABM) at 3.2 eV and the high-energy knee (HEK) at 3.4 eV. Previously we have discussed if these are vibronic structure on the absorption band.⁶ They are equally spaced in

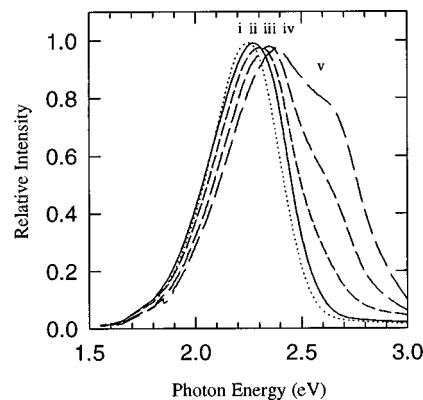


FIG. 4. Emission spectra of poly(*p*-pyridine) as a function of CSA doping level: (i) 0%, (ii) 25%, (iii) 50%, (iv) 75%, and (v) 100% CSA content.

energy and would correspond to a vibrational splitting of ~ 200 meV, corresponding to a C=C bond or CCN bond vibration. The HEK also corresponds with the position of the absorption maximum of PPY in formic acid solution, although in solution no structure is observed on the absorption band. We note that PPY is a rigid rod polymer and as such is likely to form highly ordered films.

Upon initial protonation with CSA (25%) the entire band broadens slightly and shifts to lower energy; the onset of the absorption band red-shifts by ~ 100 meV. Increasing the doping level causes a monotonic decrease in the intensity of the LES. The ABM blue-shifts and ends up close to the position of the HEK in pristine PPY. The HEK feature disappears in the highly doped samples. At 100% CSA level, the spectrum is featureless and corresponds very well to the absorption spectrum of PPY in formic acid solutions.

The corresponding normalized (to peak value) PL spectra are shown in Fig. 4, again including that of the pristine PPY film (note there is no evidence of residual protonation by formic acid in such films) for comparison. 25% and 50% CSA doping simply cause a small blue-shift in the broad featureless PL spectrum. However, at 75% and 100% a new feature grows in at ~ 2.7 eV. This corresponds to the position of the peak of the PL spectrum of PPY in formic acid solution, and mirrors what we have seen when we “dilute” PPY in PMMA.⁹ At 100% CSA content, the emission from the film appears blue-white to the eye. The measured values of the corresponding PL quantum efficiencies are shown in Fig. 5. For reference the pristine PPY film yields a value of $37 \pm 3\%$. 25% and 50% CSA have little effect on this value, whereas 75% and 100% drop it to $\sim 22\%$, still a very respectable value, especially for white emission.

B. PPY:AMPSA

The absorption spectra of PPY as a function of AMPSA level are shown in Fig. 6. Very similar behavior to CSA is observed with this acid, except at 100% AMPSA where the spectrum retains a small LES and the ABM is not blue-shifted as far as in the CSA case. The shift of the ABM as a function of increased doping level is clearly seen to be a monotonic progression as opposed to a shift of oscillator strength from one “vibronic” to another.

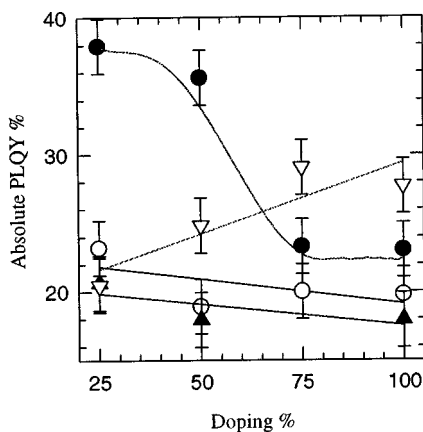


FIG. 5. Poly(*p*-pyridine) photoluminescent quantum yield as a function of acid doping level for the five acids used in this study; ● CSA, ▽ AMPSA, ○ DCA, and ▼ *m*-cresol.

The behavior of the PL spectra with doping is shown in Fig. 7. Again the behavior is similar to that with CSA, however, again at 100% the situation is a little different. A new feature appears, but at 2.55 eV, not at the characteristic solution state PL spectral maximum. This we have to ascribe to a new emission site. The behavior of the PL quantum yield is very different to CSA. 25% AMPSA reduces the quantum yield to 20% but increasing the amount of added AMPSA increases the quantum yield to a value of 28% at 100% doping, Fig. 5. This increase in PL quantum yield corresponds to the formation of the new emission feature at 2.55 eV. To the eye, the emission appears blue-white.

C. PPY:DCA

With increasing levels of DCA, the absorption band (ABM) blue-shifts by ~ 200 meV and becomes featureless, the LES disappears at high doping levels, Fig. 8. The films also appear more scattering to the eye, accounting for the apparent rise in the absorption in the 4 to 5 eV range. DCA has very little effect on the PL spectrum of PPY, a slight red-shift ~ 100 meV is all that is seen, Fig. 9. However, the PL quantum yield is reduced to $\sim 20\%$ independent of the protonation level, Fig. 5.

D. PPY:*m*-cresol

The *m*-cresol doped films show the biggest difference as compared to CSA. At first sight the complete absorption band appears to monotonically blue-shift with increasing *m*-cresol content, Fig. 10. Closer inspection shows that the relative intensity ratios of the ABM and HEK feature reverses. At 100% *m*-cresol level, the HEK is clearly the dominant feature in the spectrum although the other two features are still clearly resolved. The relative intensities of the LES and the ABM appear to remain constant. Again some increase in scattering is also seen. The changes in the PL spectra are not quite so dramatic. The spectra are blue-shifted slightly by ~ 100 meV and a new feature is seen to the high-energy side of the PL band, Fig. 11. It is not well resolved and appears here as a shoulder and does not correspond to the new fea-

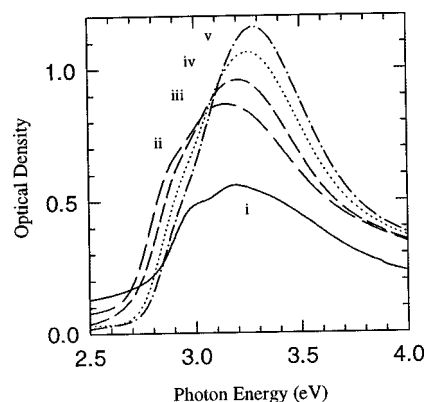


FIG. 6. Absorption spectra of poly(*p*-pyridine) as a function of AMPSA doping level: (i) 0%, (ii) 25%, (iii) 50%, (iv) 75%, and (v) 100% AMPSA content.

ture seen at high AMPSA doping levels. The PL quantum yield is constant with doping level, and reduced to $\sim 20\%$, as with DCA Fig. 5.

IV. DISCUSSION

Before discussing the obvious phenomena we have observed, a note on further work in progress is given which is very important in aiding our interpretation of the above spectroscopic data. XPS studies have determined that both CSA and AMPSA protonate PPY films whereas DCA and *m*-cresol do not.¹⁴ Further, along with protonation there is a second dopant induced interaction at the nitrogen sites as two doping induced features are observed in the *N1s* XPS spectra. This *N1s* feature is tentatively ascribed to hydrogen bonding between the protonated nitrogen sites and the carbonyl moieties on the acid counter ions.

Taking the DCA and *m*-cresol results first. With these dopants we see little shift in the emission spectrum, but relatively large redistribution of oscillator strength between the observed features on the absorption band. In both cases, however, the PL quantum yield drops markedly, even though XPS indicates no obvious protonation occurs in the films. Turning to CSA and AMPSA, both of which do protonate the PPY. Taking CSA first, increased doping leads to loss of

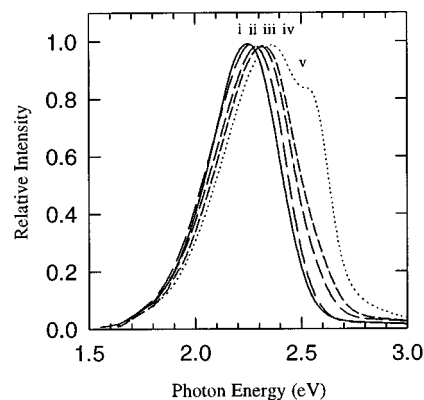


FIG. 7. Emission spectra of poly(*p*-pyridine) as a function of AMPSA doping level: (i) 0%, (ii) 25%, (iii) 50%, (iv) 75%, and (v) 100% AMPSA content.

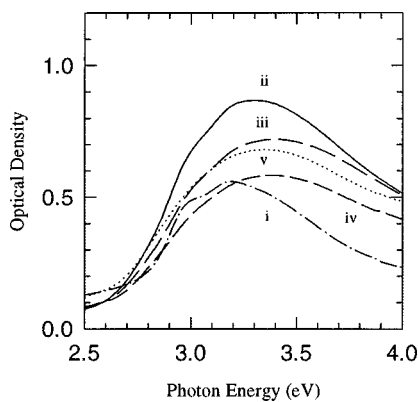


FIG. 8. Absorption spectra of poly(*p*-pyridine) as a function of DCA doping level: (i) 0%, (ii) 25%, (iii) 50%, (iv) 75%, and (v) 100% DCA content.

all structure on the absorption spectrum; at 100% the spectrum looks very characteristic of the PPY solution spectrum. This behavior is mirrored in the emission spectra where, at the highest doping level the characteristic “blue,” solution state emission is clearly seen along with the “green,” solid-state emission. We have previously observed similar behavior in our solid-state dilution studies.⁹ As the blue emission appears the PL quantum yield drops, from that of the pristine PPY film level to approximately half that value, again mirroring the solution state and dilution behavior. AMPSA behaves in much the same way in terms of absorption, although we note that at the higher doping levels the single absorption feature lies between the ABM and HEK feature of the pristine polymer. In emission, again we see a blue-shift and formation of a new high-energy feature at the highest doping levels, however, this new feature does not correspond with the solution state emission. Unlike CSA, initial doping decreases the PL quantum yield but at the highest levels it rises again, which corresponds to the observation of the new feature in the emission spectrum. These subtle differences between CSA and AMPSA could very well be due to differences in the hydrogen bonding between the PPY and respective acid counter ion.

Considering the observed changes to the ground-state absorption, there are clear differences between the absorption spectrum of the solid and solution. Structure can be seen in

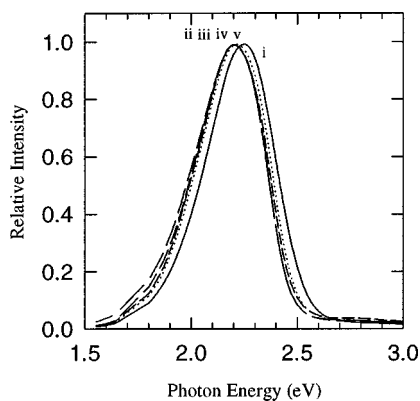


FIG. 9. Emission spectra of poly(*p*-pyridine) as a function of DCA doping level: (i) 0%, (ii) 25%, (iii) 50%, (iv) 75%, and (v) 100% DCA content.

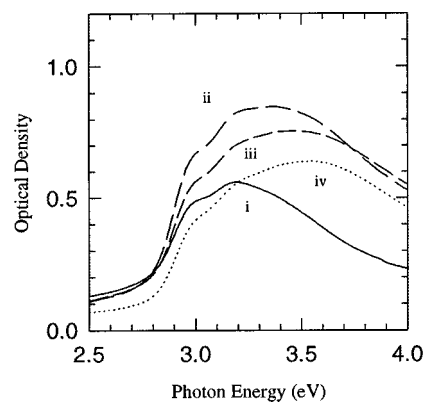


FIG. 10. Absorption spectra of poly(*p*-pyridine) as a function of *m*-cresol doping level: (i) 0%, (ii) 25%, (iii) 50%, and (iv) 100% *m*-cresol content.

the solid-state spectra but not in solution. Knowing that the polymer is a rigid rod and highly crystalline, we assume that the chains will readily pack and crystallize during film formation; note however, that spinning is a rapid drying process so that crystallization may well be lower than that observed in as synthesized powder. Therefore, we ascribe the structure on the absorption band to a vibronic progression, also these features do sharpen at low temperature. The features are equally spaced in energy, ~ 200 meV, which corresponds to a C=C or CCN stretch energy, very characteristic of conjugated polymers.²¹ As many features are observed we are not observing the formation of a simple “aggregate band” on the edge of the main absorption band. We should point out that the term aggregate has in the past been used in a very broad sense, implying that the ground state of the system extends over more than one molecule i.e., is more delocalized than would be on one chain. In many cases protonation causes a loss of this structure but no concomitant solution state, blue emission is observed, only a reduction in PLQY. DCA doping is very characteristic of this behavior whereas with *m*-cresol doping the vibronic structure is retained, again no solution state emission is observed yet the PLQY drops. This conclusion is further strengthened by our findings on the PL and PLQY properties of (pristine) PPY films and solutions.

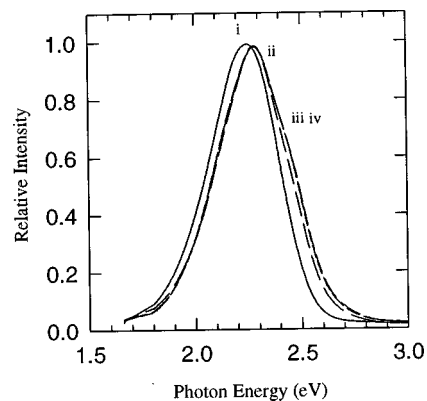


FIG. 11. Emission spectra of poly(*p*-pyridine) as a function of *m*-cresol doping level: (i) 0%, (ii) 25%, (iii) 50%, and (iv) 100% *m*-cresol content.

As already stated, calculations show that the simple act of protonation does not affect the π states of the chain, whereas our observations show this not to be the case. However, the effects we observe may not be directly attributable to an interaction between the protonation site and the chain π electrons. Thus the main observations from this present work that need to be explained are the observed changes to quantum yield and shifts in the absorption and emission spectra. Generally, addition of aromatic solvents to conjugated molecules leads to a reduction of the PLQY via the interaction between the two π systems.²² Changes in internal quenching will also affect quantum yield. Self absorption is not an issue here as the emission band is far from the absorption band edge. However, small changes to the chain geometry could affect the intersystem crossing rate (ISC). Blatchford *et al.*¹⁵ have calculated that increasing the inter-ring torsion angle along the PPY backbone will lead to mixing of the π and n orbitals which very efficiently leads to ISC and triplet formation, reducing PLQY. All of these facts lead us on to a new conclusion.

In the solid-state, interchain interactions will force the PPY backbone into its most planar configuration, i.e., lowest ring torsion angle geometry. The more planar the chain, the more delocalized the π electrons, the lower the energy gap between the HOMO and LUMO levels (or $\pi \rightarrow \pi^*$ band gap) yielding red-shifted absorption and emission. Upon addition of CSA and AMPSA the interchain interactions are reduced allowing the pyridine rings to revert back to a more twisted (lower energy) geometry. This will widen the band gap and shift the emission band to higher energy. It will also lead to greater triplet formation via increased ISC and so reduce the PL quantum yield, as we observe on addition of CSA and AMPSA or in solution (formic acid). Note that calculations indicate that a torsion angle of 30° to 35° yields the lowest energy geometry for an isolated PPY chain.¹⁶

The change from solid-statelike properties to those of the solution state upon doping will occur smoothly and monotonically for ground-state properties e.g., absorption. For emission this will not be the case as the excitation energy or exciton can migrate after creation and find the lowest energy state from which emission will occur. In the case of PPY the lowest energy state will be the chains, or portions of chains, which have the greatest delocalization. These will be the most planar regions. Once at these sites the excitons will be effectively trapped. Hence the density of such low-energy traps has to be reduced greatly before exciton migration to them is reduced to such a level that not all the excitons can find the traps before they recombine radiatively. This case will only occur at the highest doping levels or in solution, as we observe experimentally, and similarly explains why the PLQY does not decrease smoothly with increasing protonation. If, as suggested by XPS, hydrogen bonding occurs alongside protonation we can account for the subtle differences between the effects of CSA and AMPSA by the fact that AMPSA is a complex acid, containing an amide moiety. Therefore, any hydrogen bonding will be affected by the proximity of the AMPSA amide functionality to its carbonyl group. It is not obvious what role is played by either DCA or *m*-cresol. As they predominantly quench PLQY one assumes

that some kind of solvent–solute quenching mechanism must be responsible.

The absorption spectra of both CSA and AMPSA samples also show changes in intensity as a function of doping. Film thickness measurements, using an α -step profilometer, on the CSA series of samples indicate that the 25% and 50% films are of roughly equal thickness, ~ 300 nm, whereas the 75% film is thicker at ~ 400 nm. This difference is greater than experimental error. The 100% doped film was found to be too soft to measure. This indicates two things. Firstly, the differences in absorption intensity are due to different film thickness; we assume that addition of the acid changes the solution viscosity which greatly affects film thickness on spinning. Secondly, the softness of the 100% CSA film clearly shows that interchain interactions are greatly reduced either by the doping process, or as a consequence of plasticization caused by the CSA. This observation strongly supports our hypothesis that the breaking of interchain interactions is what leads on to the changes in the absorption and emission spectra of PPY allowing a direct comparison to be made between solution state and doped state behavior.

V. SUMMARY

The photophysical properties of protonated PPY have been studied and, along with previous results on the pristine polymer, a model has been put forward to explain the experimental observations. Strong, functionalized sulphonic acids such as CSA and AMPSA protonate the PPY in the solid state. Increasing the CSA protonation level leads to loss of all structure on the absorption spectrum, at 100% the spectrum looks very characteristic of the PPY solution spectrum. This behavior is mirrored in the emission spectra where at the highest doping level the characteristic blue, solution state emission is clearly seen along with the green, solid-state emission. We previously observed similar behavior in solid-state dilution studies. As the blue emission appears the PL quantum yield drops, from that of the pristine PPY film level to half that value, again mirroring the solution state and dilution behavior. AMPSA behaves in much the same way in terms of absorption, although we note that at the higher doping levels the single absorption feature blue-shifts less than in the CSA case. In emission, again we see a blue-shift and formation of a new high-energy feature as doping level increases, however, this new feature does not correspond with the solution state emission. Unlike CSA, initial doping decreases the PL quantum yield but at the highest levels a small increase is observed, which corresponds with the observation of the new feature in the emission spectrum. These small differences could be due to differences in hydrogen bonding between PPY and the respective acid counter ion. Weaker acids such as DCA and *m*-cresol cause only small shifts in the emission spectrum, but relatively large redistribution of oscillator strength between the observed features in the absorption spectra. In both cases, however, the PL quantum yield drops markedly, even though XPS indicates no protonation occurs in the films. This may be the result of solvent–solute quenching, although at present we do not fully understand the subtle interactions at work here.

The observed structure on the absorption band in the solid state is ascribed to a vibronic progression, of energy spacing ~ 200 meV. The shifts in both absorption onset and emission energy going from solid to solution state are ascribed to increasing pyridyl ring torsion angle in going from the solid state to isolated PPY chains. In the solid, interchain interactions will drive the chains to a more planar configuration, thus lowering the band gap and emission energy. On protonation, these interactions will be modified allowing the chains to relax back to their equilibrium torsion angle geometry of $\sim 30^\circ$. Increased torsion angle causes mixing of the n and π orbitals, increasing intersystem crossing and triplet formation. This causes the observed reduction in the PL quantum efficiency in highly doped samples and the solution state.

The one remaining fact that we are still unclear on is why there is such a large apparent Stokes shift between absorption and emission in both solution and solid state. Considering all the experimental evidence rules out the simple excimer or aggregate arguments. Ring torsion can explain the shifts between solution and solid-state properties, but not the initial Stokes shift. If the exciton binding energy is large in PPY, this could account for the large shift. This problem will be discussed in a further paper.

These results do, however, show how important the ring torsion degree of freedom is in heteroatomic (especially nitrogen containing) conjugated polymer systems and that much of the physics of these polymers is dominated by this degree of freedom.

ACKNOWLEDGMENTS

We would like to thank the EPSRC for ROPA Grant No. GR/K92207 to fund this work. M. Halim is a Physics Department PhD Fellow, I. D. W. Samuels is a Royal Society University Fellow. A.P.M. would like to thank the Swedish Foundation for International Cooperation in Research and Higher Education for a Fellowship and Professor W. Salaneck and the group in Linköping. Thanks also to Professor H. Burrows for such enlightening discussion and wine.

- ¹J. H. Burroughes, D. D. C. Bradley, A. R. Brown, R. N. Marks, K. Mackay, R. H. Friend, P. L. Burn, and A. B. Holmes, *Nature (London)* **347**, 539 (1990).
- ²W. J. Feast and R. H. Friend, *J. Mater. Sci.* **25**, 3796 (1990).
- ³T. Yamamoto, Y. Hayashi, and A. Yamamoto, *Bull. Chem. Soc. Jpn.* **51**, 2091 (1978); and T. Yamamoto, T. Maruyama, Z.-H. Zhou, T. Ito, T. Fukuda, Y. Yoneda, F. Begum, T. Ikeda, S. Sasaki, H. Takezoe, A. Fukuda, and K. Kubota, *J. Am. Chem. Soc.* **116**, 4832 (1994).
- ⁴M. Halim, I. D. W. Samuel, E. Rebourt, and A. P. Monkman, *Synth. Met.* **84**, 951 (1997).
- ⁵D. D. Gebler, Y. Z. Yang, J. W. Blatchford, S. W. Jessen, L.-B. Lin, T. L. Gustafson, H.-L. Wang, T. M. Swager, A. G. MacDiarmid, and A. J. Epstein, *Appl. Phys.* **78**, 4264 (1995).
- ⁶A. P. Monkman, M. Halim, S. Dailey, I. D. W. Samuel, M. Sluch, and L. E. Horsburgh, *SPIE Proc.* **3148**, 82 (1997).
- ⁷J. W. Blatchford, S. W. Jessen, L.-B. Lin, J. J. Lin, T. L. Gustafson, A. J. Epstein, D. K. Fu, M. K. Marsella, T. M. Swager, A. G. MacDiarmid, S. Yamaguchi, and H. Hamaguchi, *Phys. Rev. Lett.* **76**, 1513 (1996).
- ⁸R. L. Barnes and J. B. Birks, *Proc. R. Soc. London, Ser. A* **291**, 570 (part X) (1966).
- ⁹A. P. Monkman, M. Halim, S. Dailey, I. D. W. Samuel, and L. E. Horsburgh, *Synth. Met.* (to be published).
- ¹⁰Y. Cao and P. Smith, *Synth. Met.* **69**, 187 (1995).
- ¹¹E. R. Holland, S. J. Pomfret, P. N. Adams, and A. P. Monkman, *J. Phys.: Condens. Matter* **8**, 2991 (1996).
- ¹²L. Abell, P. N. Adams, and A. P. Monkman, *Polym. Commun.* **37**, 5927 (1996).
- ¹³O. T. Ikkala, L. Pietila, L. Ahjopalo, H. Osterholm, and P. J. Passiniemi, *J. Chem. Phys.* **22**, 9855 (1995).
- ¹⁴A. P. Monkman (to be published).
- ¹⁵J. W. Blatchford, T. L. Gustafson, and A. J. Epstein, *J. Chem. Phys.* **105**, 9214 (1996).
- ¹⁶G. Grezsinzki, N. Johanssen, A. P. Monkman, and W. J. Salaneck (to be published).
- ¹⁷M. Tiecco, L. Testaferri, M. Chianelli, and M. Montanucci, *Synth. Commun.* **1984**, 736.
- ¹⁸J. W. Blatchford, S. W. Jessen, L.-B. Lin, T. L. Gustafson, A. J. Epstein, D.-K. Fu, H.-L. Wang, T. M. Swager, and A. G. MacDiarmid, *Phys. Rev. B* **54**, 9180 (1996).
- ¹⁹L. E. Horsburgh, H. Burrows, P. N. Adams, and A. P. Monkman (to be published).
- ²⁰N. C. Greenham, I. D. W. Samuel, G. R. Hayes, R. T. Phillips, Y. A. R. Kessener, S. C. Morati, A. B. Holmes, and R. H. Friend, *Chem. Phys. Lett.* **241**, 89 (1995).
- ²¹E. R. Holland, D. Bloor, A. P. Monkman, A. Brown, D. De Leeuw, M. M. Bouman, and E. W. Meijer, *J. Appl. Phys.* **75**, 7954 (1994).
- ²²J. B. Birks, A. A. Kazzaz, and T. A. King, *Proc. R. Soc. London, Ser. A* **291**, 556 (1966).